

ORIGINAL ARTICLE

CDK5-dependent inhibitory phosphorylation of Drp1 during neuronal maturation

Bongki Cho¹, Hyo Min Cho¹, Hyun Jung Kim¹, Jaehoon Jeong², Sang Ki Park², Eun Mi Hwang³, Jae-Yong Park^{3,4}, Woon Ryoung Kim¹, Hyun Kim¹ and Woong Sun¹

Mitochondrial functions are essential for the survival and function of neurons. Recently, it has been demonstrated that mitochondrial functions are highly associated with mitochondrial morphology, which is dynamically changed by the balance between fusion and fission. Mitochondrial morphology is primarily controlled by the activation of dynamin-related proteins including dynamin-related protein 1 (Drp1), which promotes mitochondrial fission. Drp1 activity is regulated by several post-translational modifications, thereby modifying mitochondrial morphology. Here, we found that phosphorylation of Drp1 at serine 616 (S616) is mediated by cyclin-dependent kinase 5 (CDK5) in post-mitotic rat neurons. Perturbation of CDK5 activity modified the level of Drp1^{S616} phosphorylation and mitochondrial morphology in neurons. In addition, phosphorylated Drp1^{S616} preferentially localized as a cytosolic monomer compared with total Drp1. Furthermore, roscovitine, a chemical inhibitor of CDKs, increased oligomerization and mitochondrial translocation of Drp1, suggesting that CDK5-dependent phosphorylation of Drp1 serves to reduce Drp1's fission-promoting activity. Taken together, we propose that CDK5 has a significant role in the regulation of mitochondrial morphology via inhibitory phosphorylation of Drp1^{S616} in post-mitotic neurons.

Experimental & Molecular Medicine (2014) 46, e105; doi:10.1038/emm.2014.36; published online 11 July 2014

Keywords: CDK5; Drp1; fission; mitochondria; neuron; phosphorylation

INTRODUCTION

Mitochondria support the development, function and survival of neurons by synthesizing ATP, maintaining intracellular calcium and regulating the release of apoptotic proteins such as cytochrome *c* and apoptosis-inducing factor from the mitochondrial inter-membrane space.^{1,2} Recent reports have demonstrated that the regulation of mitochondrial morphology is involved in several cellular physiologies and pathologies.³ For example, cells that are exposed to mild stressors⁴ or starvation,^{5,6} as well as cells undergoing cellular senescence,⁷ exhibit elongated mitochondria. Elongation of mitochondria appears to protect the cells by promoting ATP synthesis and preventing mitochondrial autophagy.^{5,8} Conversely, apoptotic stimuli induce mitochondrial fragmentation, which accelerates mitochondrial outer-membrane permeabilization, resulting in cell death.^{9,10}

Mitochondrial morphology is determined by continuous fusion and fission, which are regulated by large GTPase dynamin-related proteins, including Mitofusin 1/2 (Mfn1/2),

Optic atrophy 1 (Opa1) and Dynamin-related proteins 1 (Drp1).³ Whereas Mfn1/2 and Opa1 promote fusion between adjacent mitochondria,¹¹ Drp1 is recruited into mitochondria by mitochondrial receptors, including Fis1 and Mff,¹² and induces mitochondrial fission by forming high-ordered spiral structure on the mitochondrial outer membrane, followed by GTP hydrolysis.^{13,14} Especially in neurons, Drp1-mediated mitochondrial fission is required for several physiologies, including development of nervous system,^{15,16} synaptic plasticity¹⁷ and normal programmed cell death.¹⁸

Drp1 activity is regulated by several post-translational modifications including phosphorylation.¹⁹ Specifically, serine 616 of Drp1 can be phosphorylated by multiple kinases on specific cellular conditions.²⁰ For example, Drp1 is phosphorylated at serine 616 (S616) by cyclin-dependent kinase 1 (CDK1) during mitosis, resulting in mitochondrial fragmentation for even transfer of mitochondria into two daughter cells.^{21,22} In addition, ERK1/2 and PKC δ

¹Department of Anatomy, College of Medicine, Korea University, Seoul, Republic of Korea; ²Department of Life Science, Pohang University of Science and Technology, Pohang, Gyungbuk, Republic of Korea; ³Center for Neural Science and WCI Center for Functional Connectomics, Korea Institute of Science and Technology, Seoul, Republic of Korea and ⁴Department of Physiology, Institute of Health Science, School of Medicine, Gyeongsang National University, Jinju, Republic of Korea

Correspondence: Professor W Sun, Department of Anatomy, College of Medicine, Korea University, Seoul 136-701, Republic of Korea.

E-mail: woongsun@korea.ac.kr

Received 12 December 2013; revised 1 March 2014; accepted 26 March 2014

phosphorylate Drp1^{S616} thereby inducing mitochondrial fragmentation under pathological conditions, including hyperglycemia and oxidative stress, respectively.^{23,24} However, post-mitotic neurons do not exhibit substantial CDK1 activity in physiological conditions,²⁵ and it is unclear whether Drp1 activity is regulated by phosphorylation at serine 616 by other upstream kinase(s) in neurons. CDK1 and CDK5 share the same consensus site for phosphorylation, and post-mitotic neurons have high level of CDK5,²⁶ but not CDK1,²⁵ activity in physiological conditions. A recent report has demonstrated that CDK5 can phosphorylate Drp1^{S616},²² raising the possibility that CDK5 may regulate Drp1 activity by phosphorylation at serine 616 in post-mitotic neuron. However, the molecular link between Drp1 and CDK5 and its physiological role in neuronal cells have not been fully clarified.

In this study, we found that post-mitotic mature neurons exhibit high levels of phosphorylated Drp1^{S616}, and this phosphorylation is, at least partly, mediated by CDK5 activation. Furthermore, CDK5-dependent phosphorylation of Drp1 in neurons serves as an inhibitory modification of Drp1 activity, providing evidence for the novel role of CDK5 in the regulation of mitochondrial morphology.

MATERIALS AND METHODS

Primary neuron and HeLa cell culture, gene transfection and reagents

Primary neuron cultures were prepared as previously reported.²⁷ In brief, the cortical or hippocampal regions were separated, trypsinized and dissociated into single neurons from rat embryos (embryonic day 16, E16). This experiment was carried out in strict accordance with the recommendations in the Guide for the Care and Use of Laboratory Animals of the Korea University Institutional Animal Care and Use Committee. The protocol was approved by the Committee on the Ethics of Animal Experiments of the Korea University (Permit Number: KUIACUC20110304-2). Rats were killed under isoflurane anesthesia to minimize suffering. The neurons were plated onto glass coverslips coated with poly-D-lysine (Sigma-Aldrich, St Louis, MO, USA) at 10^5 cells cm^{-2} (cortical neurons) or 0.5×10^5 cells cm^{-2} (hippocampal neurons), and maintained in 5% CO_2 at 37 °C with neurobasal media (Gibco, Grand Island, NY, USA) containing 2% B27 supplement (Gibco), 200 mM L-glutamine (Gibco), 0.5 mM L-glutamate (Gibco) and 1% penicillin/streptomycin (Gibco). After 2 days *in vitro* (DIV2), the cells were placed in neurobasal media lacking L-glutamate and maintained as needed. For gene transfection into cultured neurons, the Calphos mammalian transfection kit (Clontech, Mountain View, CA, USA) was used according to the manufacturer's protocol. Transfection into the cultured neurons was performed 2 days (DIV2 or DIV8) before experimental observation (DIV4 or DIV10). HeLa cells were maintained in 5% CO_2 at 37 °C. For gene transfection into HeLa cells, Lipofectamine 2000 reagent (Invitrogen, Carlsbad, CA, USA) was used according to the manufacturer's protocol. Roscovitine (EMD Millipore, Billerica, MA, USA), PD98059 (EMD Millipore) and Bisindolylmaleimide I (EMD Millipore) were solubilized in DMSO.

DNA constructs

DsRed-mito was purchased from Clontech. CDK5-GFP and p25-GFP were created by inserting polymerase chain reaction (PCR)-isolated

human CDK5 and p25 cDNA into the pDEST-GFP-XB vector, which was modified from pEGFP-N1 (Clontech) using the Gateway system. DN-CDK5-GFP, a dominant-negative CDK5 fused to GFP, was generated by single-nucleotide mutagenesis of D144 to N144 in CDK5-GFP. To produce YFP-hDrp1, we inserted the human *Drp1* gene from pcDNA-hDrp1⁹ into the pEYFP-C1 vector (Clontech). Two mutants, YFP-hDrp1(S616A) and YFP-hDrp1(S616D), were produced by mutagenesis using the PCR primers 5'-ATT ATG CCA GCC GCT CCA CAA AAA GGT-3' and 5'-ATT ATG CCA GCC GAT CCA CAA AAA GGT-3', respectively (underlined sequences represent mutation sites). For DN-Drp1, we cloned the PCR product from pcDNA-hDrp1(K38A)⁹ into the pIRES2-DsRed-mito vector, which was modified from pIRES2-GFP (Clontech) by exchanging GFP with DsRed-mito using PCR.

Immunohistochemistry, immunocytochemistry and measurement of mitochondrial length

Immunohistochemical analyses were performed as previously reported.²⁸ In brief, rats were deeply anesthetized and then perfused with 4% paraformaldehyde. Following post-fixation in the same fixative overnight, isolated brains were cryo-protected in 30% sucrose and sectioned serially (40 μm). The following primary antibodies were applied overnight at 4 °C: anti-Drp1 (BD Biosciences, San Jose, CA, USA, #611112; 1:500), anti-pDrp1^{S616} (Cell Signaling, Beverly, MA, USA, #3455; 1:500), anti-CDK5 (Santa Cruz Biotechnology, Santa Cruz, CA, USA, #sc-6247; 1:500), anti-p35 (Cell Signaling, #2680; 1:300) and anti-NeuN (EMD Millipore, #MAB377; 1:1000). After several washes with PBS, appropriate secondary antibodies were applied for 1 h. Subsequently, sections were washed, mounted and observed with a confocal microscope (Carl Zeiss LSM 510 or LSM 700). Hoechst 33342 dye was used for the counterstaining of nuclei. For immunocytochemistry, cultured neurons and HeLa cells were fixed with 4% paraformaldehyde and washed by PBST. The following primary antibodies were then applied for 2 h at 25 °C: anti-Drp1 (1:100), anti-pDrp1^{S616} (1:100) and anti- α -tubulin (Santa Cruz Biotechnology, #sc-8035; 1:500). After several washes with PBST, appropriate secondary antibodies were applied for 1 h. Images for immunocytochemistry were also captured by confocal microscope.

We obtained images of mitochondria labeled with DsRed-mito using fluorescence microscopy (Carl Zeiss Axioskop2 Plus). We measured the length of all mitochondria (80 or more mitochondria per single neuron), which are localized in all neurites (200 μm from soma) of 10 neurons. For the measurement of mitochondrial length, we converted the mitochondrial image to a binary image with the 'threshold' module of ImageJ software (NIH), and we obtained mitochondrial length by using the 'skeletonize' and 'analyze particles' modules.

Detection of oligomeric Drp1, mitochondrial fractionation and immunoblotting

For detecting oligomeric Drp1, cultured cortical neurons were collected in lysis buffer (100 mM NaCl, 5 mM EDTA, 0.5% Triton X-100, 50 mM Tris-Cl, protease and phosphatase inhibitor cocktails, pH 7.4). Then, non-reducing SDS-PAGE was performed using samples that were either left untreated or treated with DTT (1 μM). For mitochondrial fractionation, cultured cortical neurons were rinsed with PBS and collected in pre-chilled mitochondria buffer (250 mM sucrose, 10 mM KCl, 5 mM MgCl_2 , 1 mM EDTA, 1 mM EGTA, 20 mM HEPES, protease and phosphatase inhibitor cocktails, pH 7.5,

4 °C). Supernatant was obtained by centrifugation at $500 \times g$ for 5 min and $10\,000 \times g$ for 15 min at 4 °C. The pellet and supernatant represented the mitochondrial and cytosolic fractions, respectively. Immunoblotting was performed using the following antibodies: anti-Drp1 (1:2000), anti-pDrp1^{S616} (1:500), anti-CDK5 (1:1000), anti-p35 (1:1000), anti- β -Actin (Sigma-Aldrich, #A5441; 1:2000), anti-HSP60 (Enzo Life Sciences, Farmingdale, NY, USA, #ADI-SPA-806; 1:1000), anti-GAPDH (Santa Cruz Biotechnology, #6C5; 1:1000), anti-Mfn2 (Abcam, Cambridge, MA, USA, #ab56889; 1:1000), anti-Opa1 (BD Biosciences, #612606; 1:1000), anti-Mff (Sigma-Aldrich, #HPA010968; 1:1000) and anti-Fis1 (Abcam, #ab96764; 1:1000).

Quantification of mitochondrial and genomic DNA

We extracted genomic and mitochondrial DNA from cultured neurons by using the traditional phenol/chloroform extraction method. In brief, cells were lysed in lysis buffer (50 mM Tris-Cl, pH 8.0, 0.1 M NaCl, 0.1 M mM EDTA, 1% SDS, 0.5 mg ml⁻¹ proteinase K,) at 55 °C and added one volume of phenol:chloroform:isoamyl alcohol (25:24:1). The pellet was obtained by centrifugation at full speed ($12\,000 \times g$) for 5 min, was washed by adding 70% ethanol and subsequently was centrifuged at full speed. After drying, the DNA pellet was dissolved in TE buffer (10 mM Tris-Cl, 1 mM EDTA, pH 8.0). We detected genomic and mitochondrial DNA by PCR using DNA primers. For GAPDH, which is located on the genomic locus, 5'-ATG GGA AGC TGG TCA TCA AC-3' and 5'-GGA TGC AGG GAT GAT GTT CT-3' were used. For Cox1, which is located on the genomic locus, 5'-AGC CGG GGT GTC TTC TAT CT-3' and 5'-ATA ATA TGG CGG GGG ATC AT-3' were used.

Statistical analysis

Quantitative data were analyzed using unpaired Student's *t*-test.

RESULTS

Drp1^{S616} is highly phosphorylated in post-mitotic mature neurons from the rat brain

We explored the distribution of phosphorylated Drp1^{S616} immunoreactivity in embryonic (E18.5) and adult rat brains (Figure 1). In the embryonic cerebral cortex, total Drp1 and phosphorylated Drp1^{S616} were widely distributed in the entire cerebral cortex, including cortical plates where post-mitotic neurons are enriched (Figures 1a–c). Double immunofluorescence labeling of the phosphorylated Drp1 and a mature neuronal marker, NeuN, clearly demonstrated that NeuN-expressing post-mitotic neurons in the cortical plate expressed phosphorylated Drp1^{S616} as determined by immunoreactivity (Figures 1d–f). Non-neuronal cells in the marginal zone, which do not express NeuN, also exhibited a substantial level of phosphorylated Drp1^{S616} immunoreactivity. In the adult cerebral cortex, most cells strongly expressed Drp1, while only a subset of Drp1-expressing cells also exhibited strong phosphorylated Drp1^{S616} immunoreactivity (Figures 1g–i). Double immunofluorescence labeling showed that cells exhibiting phosphorylated Drp1^{S616} are mostly neurons (Figures 1j–l). Immunoblot analysis further demonstrated the Drp1 phosphorylation in the adult cerebral cortex where virtually no cells proliferate (Figure 1m), indicating that the phosphorylation of Drp1^{S616} is evident in the post-mitotic neurons.

Phosphorylation of Drp1^{S616} is increased with mitochondrial elongation during neuronal maturation

Next, we examined the phosphorylation of Drp1^{S616} in cultured neurons. Immunocytochemical and immunoblot analyses revealed that total Drp1 and phosphorylated Drp1^{S616} are progressively increased during the neuronal maturation *in vitro* (Figures 2a–c). In addition to Drp1^{S616}, phosphorylation at serine 637 was also increased (Supplementary Figure S1a), while the expression levels of other proteins promoting mitochondrial fission and fusion, including Mfn2, Opa1 and Fis1, were not significantly different between DIV4 and DIV10 (Supplementary Figure S1b). However, the expression of Mff, a receptor for Drp1, was markedly increased, suggesting that Drp1-dependent mitochondrial fission machineries are upregulated during the neuronal maturation. To examine whether an increase in Drp1^{S616} phosphorylation is correlated with morphological change of mitochondria during neuronal maturation, we assessed mitochondrial length in neuronal processes. As previously reported,^{8,29,30} mitochondria appeared to be elongated during neuronal maturation (Figure 2d). Frequency-fractionation analysis demonstrated that a large proportion of mitochondria in mature neurons (DIV 10) exhibit elongated tubular morphology compared with young neurons (DIV4) (Figure 2e), and there was a significant increase in the average mitochondrial length (Figure 2f). In addition, we found that total mitochondrial contents were progressively increased during the *in vitro* maturation of neurons (Supplementary Figure S2). These data suggest that mitochondrial elongation during the neuronal maturation may be mediated by multiple factors including increases in the mitochondrial contents, the total Drp1 protein levels and phosphorylation of Drp1.

Phosphorylation of Drp1^{S616} is mediated by CDK5 in post-mitotic neurons

It is known that Drp1^{S616} can be phosphorylated by CDK1 in mitotic cells.^{21,22} Because post-mitotic neurons have high activity of CDK5²⁶ but no substantial CDK1 activity under physiological conditions,²⁵ we postulated that CDK5 may regulate Drp1 activity through phosphorylation of serine 616 in post-mitotic neurons. Furthermore, it was recently reported that CDK5 can directly phosphorylate Drp1.²² Supporting this idea, CDK5 and its coactivator p35/p25 were coexpressed in the cerebral cortex of adult rats (Figures 3a–c), and the expression pattern of phosphorylated Drp1^{S616} was similar to the pattern of CDK5 expression (Figures 3d–f). Next, we tested whether the suppression of CDK5 affects the phosphorylation of Drp1^{S616} in neurons. Treatment with roscovitine, an inhibitor of CDKs, reduced the level of Drp1^{S616} phosphorylation in a dose-dependent manner in mature neurons without affecting the total Drp1 (Figure 3g). We also tested other possible upstream kinases such as ERK1/2 and PKC δ . Blockade of ERK1/2 by PD98059 significantly reduced the Drp1^{S616} phosphorylation, whereas the blockade of PKC δ by Bisindolylmaleimide I (Bis-I) failed to modify Drp1^{S616} phosphorylation, suggesting that at least two kinases, CDK5

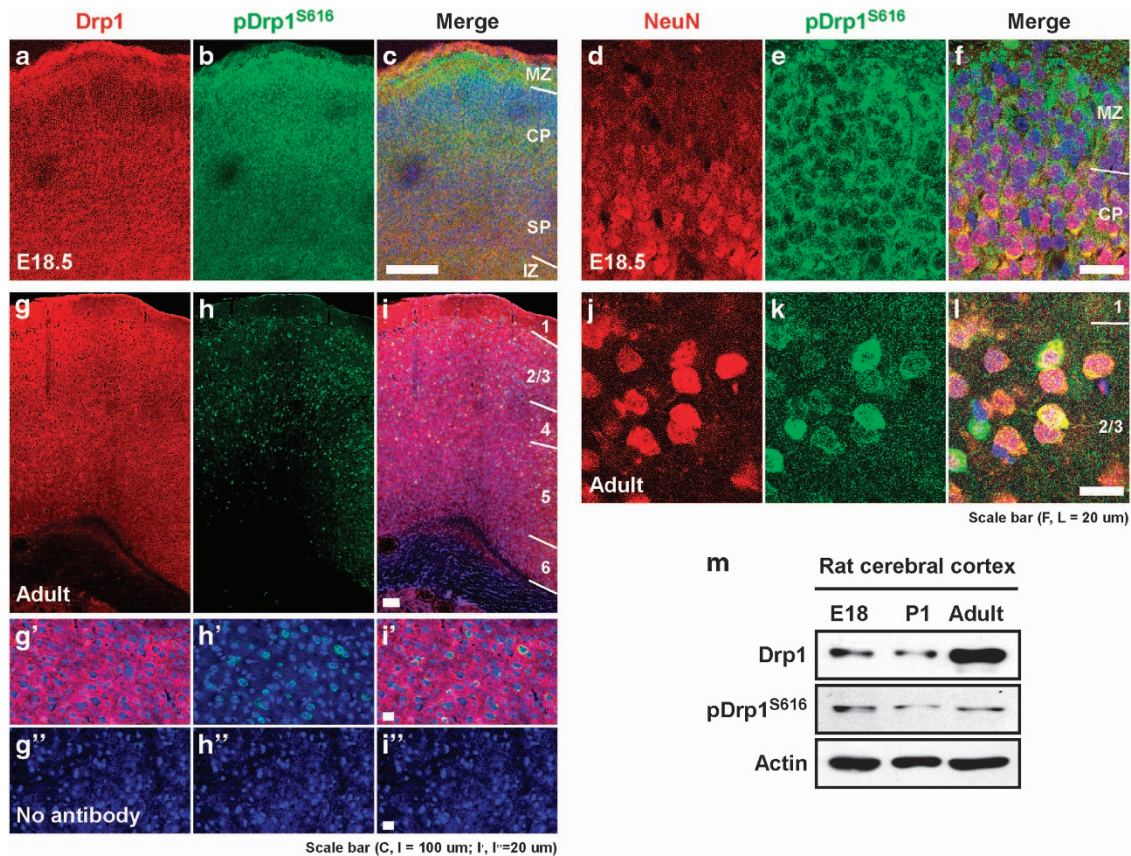


Figure 1 Enrichment of Drp1 and phosphorylated Drp1^{S616} in post-mitotic mature neurons. (a–l) Immunohistochemical labeling of Drp1 (a, g, g'), phosphorylated Drp1^{S616} (pDrp1^{S616}; b, h, h') and their merged image (c, i, i'), or NeuN (d, j) and pDrp1^{S616} (e, k) of embryonic (E18.5; a–f) and adult (g–l) rat cerebral cortex. (g', h', i') Immunohistochemical labeling without antibodies against Drp1 and pDrp1^{S616} as negative controls. CP, cortical plate; IZ, intermediate zone; MZ, marginal zone; SP, subplate. (m) Immunoblot of Drp1 and pDrp1^{S616} in embryonic (E18), post-natal (P1), and adult rat cerebral cortex.

and ERK1/2, are involved in the Drp1^{S616} phosphorylation in neurons. Contribution of CDK5 to the Drp1^{S616} phosphorylation in neurons was further confirmed by the observation that overexpression of dominant-negative mutant of CDK5 (DN-CDK5) markedly reduced the Drp1^{S616} phosphorylation in cultured neurons (Figure 3h). Furthermore, overexpression of p25 in HeLa cells increased the phosphorylation of endogenous Drp1^{S616} and exogenously expressed YFP-Drp1^{S616}, which was inhibited by cotransfection of DN-CDK5 (Figure 3i), consistent with a previous report.²² Therefore, we concluded that CDK5 regulates the phosphorylation of Drp1 in post-mitotic neurons.

CDK5 is involved in mitochondrial elongation during neuronal maturation

To examine whether CDK5 activity is correlated with mitochondrial elongation during neuronal maturation, we assessed mitochondrial morphology following perturbation of CDK5 activity. Overexpression of DN-CDK5 significantly decreased the mitochondrial length in mature neurons (Figures 4a, b and d). Similarly, roscovitine also reduced mitochondrial length in neurons (Supplementary Figure S3a, b) without affecting the levels of other proteins, such as Mfn2, Opa1, Fis1 and Mff

(Supplementary Figure S3c). Conversely, overexpression of CDK5 and p25 significantly increased mitochondrial length (Figures 4a, c and d), although this condition induced death of a subpopulation of neurons as previously reported (Supplementary Figure S4a).³¹ Surprisingly, a subset of neurons showing condensed nuclei (a hallmark of neuronal death) maintained their elongated mitochondrial morphology (Supplementary Figure S4b), implying that mitochondrial elongation by CDK5 activation may be a separate event from the CDK5-dependent cell death-promoting pathways. Overexpression of CDK5 and p35, another form of the CDK5 coactivator, also promoted mitochondrial elongation (data not shown). Next, we examined Drp1 involvement in mitochondrial shortening by coexpression of DN-CDK5 and a dominant-negative mutant of Drp1 (DN-Drp1). All DN-Drp1-expressing neurons exhibited hyper-elongated mitochondrial morphology (Figure 4e), and DN-Drp1 completely blocked mitochondrial shortening caused by DN-CDK5 (Figure 4f). In contrast to the CDK5 inhibition, blockade of ERK1/2 by PD98059 slightly elongated the mitochondrial length (Supplementary Figure S3a, b), suggesting that phosphorylation of Drp1 by these two different upstream kinases propagate opposite impact on the mitochondrial length.

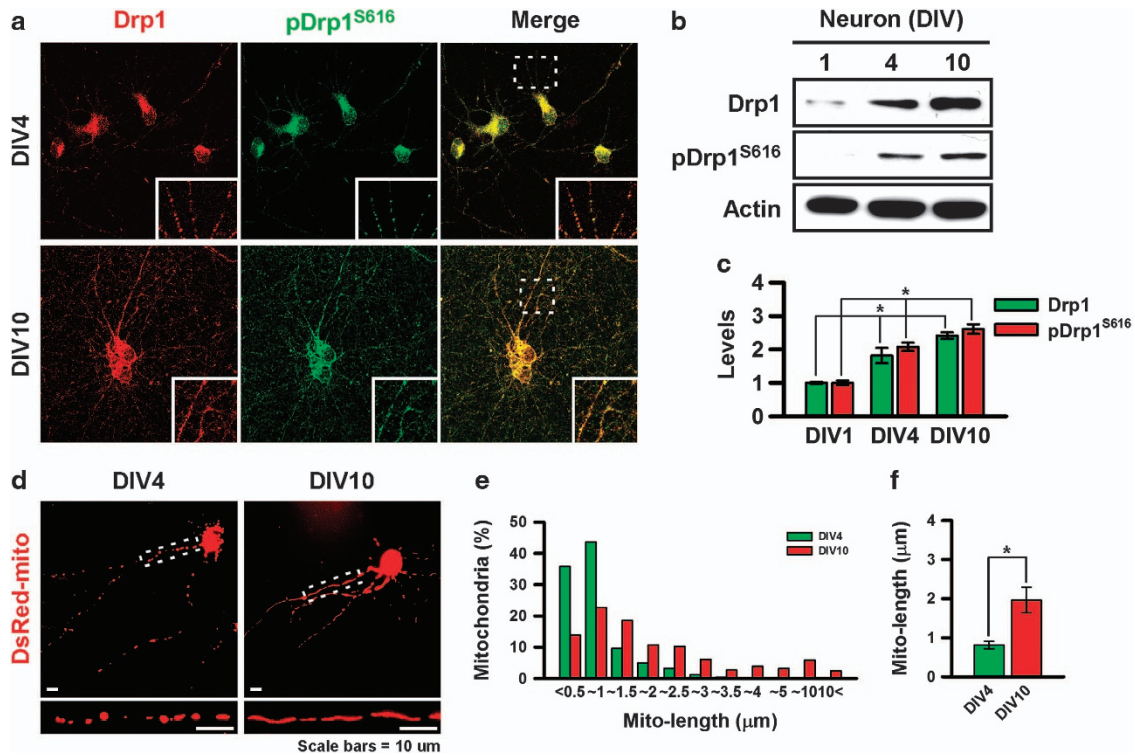


Figure 2 Phosphorylation of Drp1^{S616} and mitochondrial elongation during neuronal maturation. Immunocytochemical staining (a) and immunoblotting (b) of Drp1 and pDrp1^{S616} during the maturation of cultured cortical neurons *in vitro*. (c) Quantitative analysis of total Drp1 and pDrp1^{S616} protein levels. **P*<0.05 in Student's *t*-test comparison, *n*=3. (d) Mitochondrial morphology of cultured cortical neurons on DIV4 (left panel) or DIV10 (right panel). Mitochondria were visualized by cotransfection of a DsRed-mito plasmid (red). Large magnification images of the mitochondrial morphology in white dotted boxes are straightened by using the 'straighten' module of ImageJ and are shown at the bottom of each panel. (e) Frequency-fractionation analysis of mitochondrial length. (f) Average of mitochondrial length. **P*<0.05 in Student's *t*-test comparison, *n*=10.

Considering that, the increased phosphorylation of Drp1^{S616} is closely associated with mitochondrial elongation during the neuronal maturation, we favor the idea that CDK5 is major upstream kinase for Drp1^{S616} phosphorylation during the neuronal maturation.

Phosphorylation of Drp1^{S616} by CDK5 reduces Drp1 activity in neurons

Previous studies have reported that phosphorylation of Drp1^{S616} by CDK1 and CDK5 enhances Drp1 activity by promoting the dissociation of Drp1 from the microtubule.^{21,22} However, our current observations suggest that CDK5-dependent phosphorylation of Drp1^{S616} might suppress Drp1 activity in neurons. To address this issue, we transfected YFP-hDrp1(S616A) or YFP-hDrp1(S616D), which are phosphorylation-defective or -mimicking forms of Drp1, respectively, into neurons. A subset (21%) of wild-type YFP-hDrp1-expressing neurons exhibited extensive filamentous forms of YFP-hDrp1 signals (Figures 5c' and f), although a large population of neurons exhibited punctate forms (Figure 5b'). Interestingly, a higher proportion (35.2%) of YFP-hDrp1(S616A)-expressing neurons exhibited filamentous signals (Figures 5d' and f), which were rarely displayed by YFP-hDrp1(S616D)-expressing neurons (7.7%) (Figures 5e'

and f). Similarly, we overexpressed wild-type or phosphor-mutants of YFP-hDrp1 in HeLa cells and found punctate or filamentous forms by YFP-hDrp1 (Supplementary Figure S5a). As in neurons, a higher population of YFP-hDrp1(S616A)-expressing cells exhibited filamentous signals, but YFP-hDrp1(S616D)-expressing cells rarely showed the filaments (Supplementary Figure S5b), although expression levels of wild type and phosphor-mutants of YFP-hDrp1 were similar (Supplementary Figure S5c). These data indicate that filament formation by YFP-hDrp1 is determined by phosphorylation status of Drp1 rather than protein levels. This filamentous form of YFP-hDrp1 is a known product of excessive polymerization of Drp1 associated with microtubules.^{22,32} We also found that this filamentous form of YFP-hDrp1 was closely associated with microtubules (Supplementary Figure S5d, e). Contradictory to a previous report,²² neurons with filamentous YFP-hDrp1 exhibited excessive mitochondrial fragmentation (Figures 5c and d). Furthermore, a higher proportion of neurons expressing YFP-hDrp1(S616A) showed mitochondrial fragmentation compared with YFP-hDrp1(S616D) (Figures 5d, e and g). Therefore, these data suggest that phosphorylation of Drp1^{S616} may suppress Drp1 activity by alterations of their self-oligomerization and microtubule-binding activities in neurons.

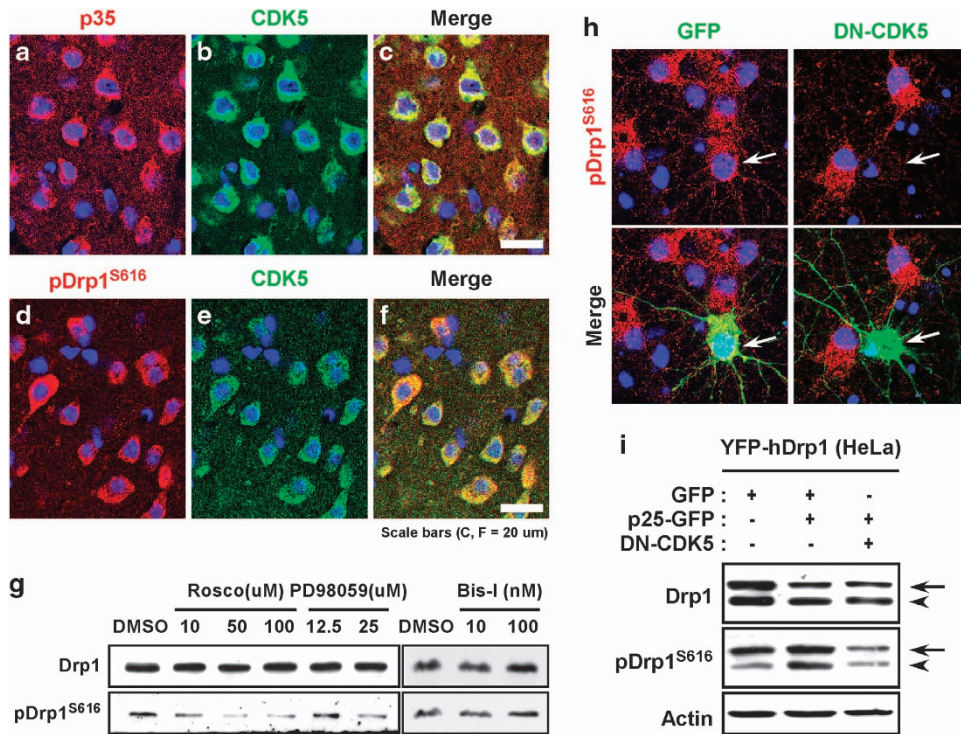


Figure 3 Phosphorylation of Drp1^{S616} is mediated by CDK5 in neurons. Immunohistochemical labeling signals of p35 (a) and CDK5 (b), or pDrp1^{S616} (d) and CDK5 (e) in adult rat cerebral cortex. A merged image is shown in c and f. Nuclei were counterstained with Hoechst 33342 (blue). (g) Immunoblot of Drp1 and pDrp1^{S616} in cultured cortical neurons (DIV10) following the treatment with different concentrations of roscovitine, PD98059 and Bisindolylmaleimide I (Bis-I) for two hours. (h) Immunocytochemical labeling of pDrp1^{S616} (red) in cultured cortical neurons transfected with GFP (left panels) or DN-CDK5-GFP (right panels). Nuclei were counterstained with Hoechst 33342 (blue). Arrows indicate cells expressing GFP or DN-CDK5-GFP. (i) Immunoblot of Drp1 and pDrp1^{S616} in HeLa cells transfected with or without GFP, p25-GFP and DN-CDK5. Arrows indicate the bands derived from transfected YFP-hDrp1 proteins, while arrowheads indicate the bands derived from the endogenous Drp1.

Phosphorylation of serine 616 inhibits oligomerization and mitochondrial translocation of Drp1 in neurons

We further tested whether the phosphorylation of Drp1^{S616} affected the oligomerizing activity and mitochondrial distribution. Non-reducing gel electrophoresis demonstrated that the majority of Drp1 exist as tetrameric forms and small fractions show monomeric or higher-ordered oligomeric forms, consistently with previous reports (Figure 6a).^{33,34} Interestingly, phosphorylated Drp1^{S616} preferentially exists in a monomeric form rather than in tetrameric or higher-ordered oligomeric forms, compared with total Drp1 (Figures 6a and b). Treatment with reducing agents such as DTT markedly dissociated the oligomeric forms, confirming that the high molecular weight bands observed correspond to the oligomeric forms of Drp1. In addition, subcellular fractionation revealed that phosphorylated Drp1^{S616} is preferentially localized in the cytosolic fraction compared with the mitochondrial fraction (Figures 6c and d). These data indicate that phosphorylated Drp1^{S616} may preferentially exist as an inactivated form. Suppression of Drp1^{S616} phosphorylation by roscovitine significantly promoted tetramerization of Drp1 (Figures 6e and f) and increased the level of Drp1 in the mitochondrial fraction (Figures 6g and h). Taken together, these results suggest that CDK5-dependent phosphorylation inhibits the oligomerizing

activity and mitochondrial translocation of Drp1 in neurons, which in turn reduces its fission-promoting activity.

DISCUSSION

In this study, we found that Drp1^{S616} can be phosphorylated in post-mitotic neurons. Although this site is phosphorylated by CDK1 during mitosis,²¹ CDK1 activity in normal post-mitotic neurons is very low because cyclin B1, activator of CDK1, is constitutively degraded by the Cdh1-APC complex in physiological condition.²⁵ Although CDK1 activity can be activated under specific pathological conditions,^{25,35} it is difficult to explain that high-level of Drp1^{S616} phosphorylation in normal mature neurons is mainly mediated by CDK1. In fact, dynamin 1, which contains similar motifs with Drp1 as an endocytotic molecule, is phosphorylated by CDK5, and it inhibits association and subsequent polymerization with amphiphysin 1,³⁶ resulting in the suppression of vesicle endocytosis.³⁷ Therefore, we postulated that Drp1^{S616} phosphorylation may be mediated by the neuron-specific kinase CDK5, having multiple physiological functions in neuronal development, synaptic plasticity and survival.²⁶ However, several reports have demonstrated that CDK5 is involved in the regulation of mitochondrial dynamics in various pathological conditions.

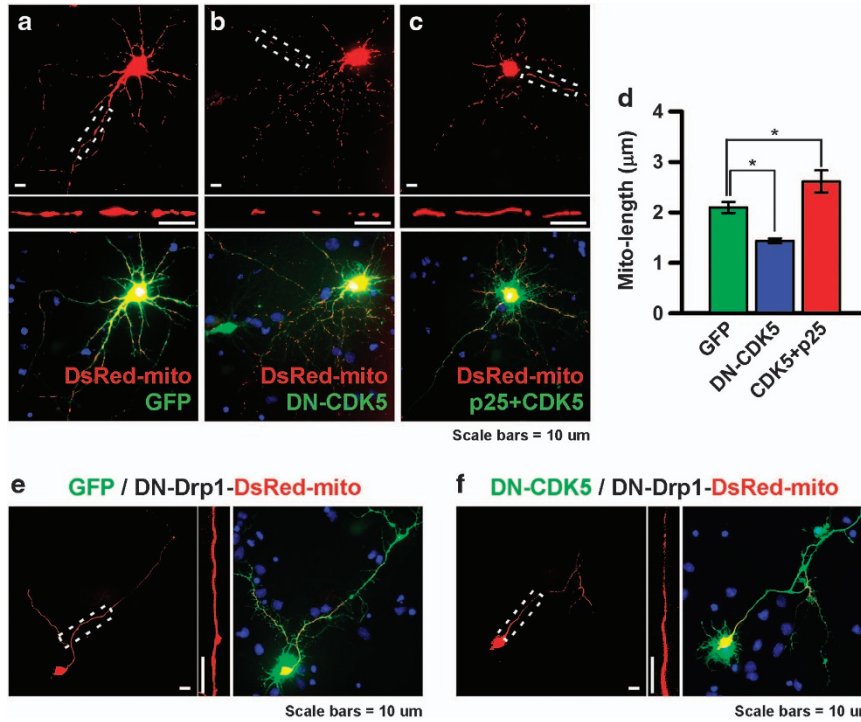


Figure 4 Perturbation of CDK5 activity induces change on mitochondrial morphology. (a–c) Mitochondrial morphology of cultured cortical neurons in GFP- (a), DN-CDK5-GFP- (b), or CDK5-GFP and p25-transfected (c) groups at DIV10. Large, straightened mitochondrial morphology in white dotted boxes of a–c are shown at the bottom of each panel. (d) Average length of the mitochondria in each group. * $P < 0.05$, $n = 10$. (e, f) Mitochondrial morphology of cortical neurons cotransfected with DN-Drp1 and GFP (e) or DN-CDK5-GFP (f). Magnified images of the mitochondrial morphology in white dotted boxes are shown on the right side of each panel.

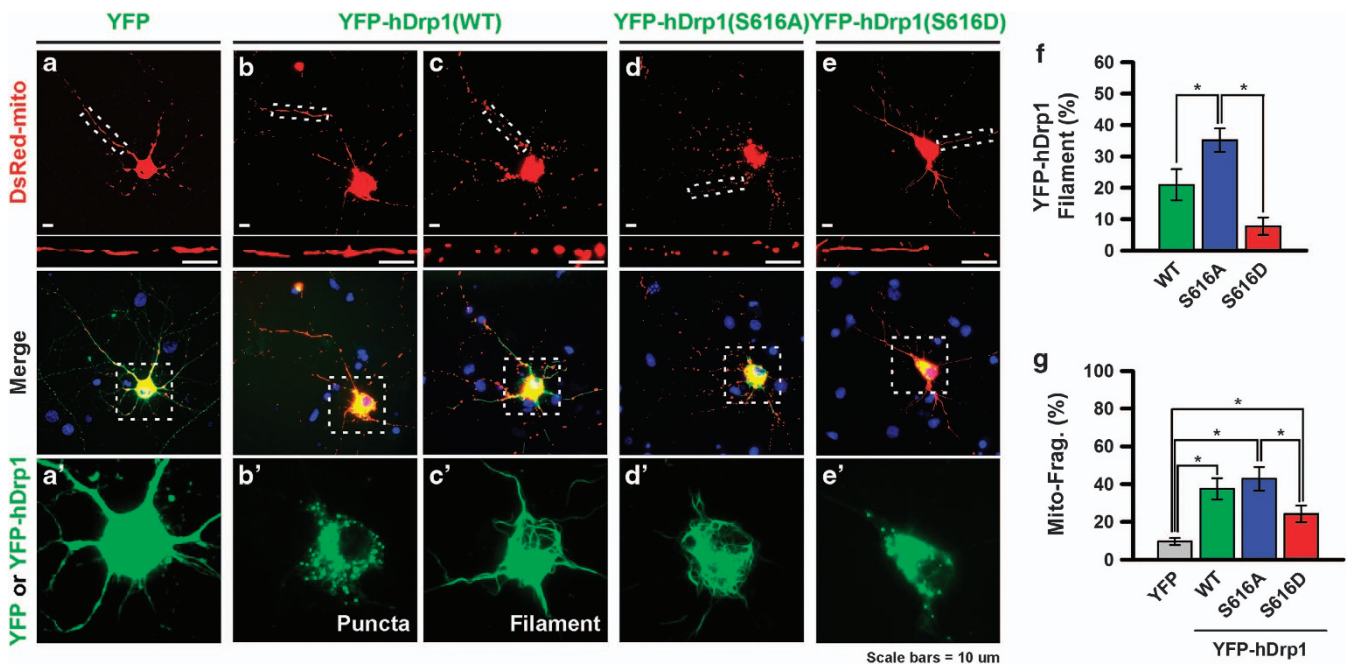


Figure 5 Phosphorylation of Drp1^{S616} modifies its oligomerization and inhibits mitochondrial fragmentation in neurons. (a–e, a'–e') Morphology of mitochondria in cells expressing YFP (a, a'), YFP-hDrp1 (b, c, b', c') or its phosphorylation mutants, which are YFP-hDrp1(S616A) (d, d') and YFP-hDrp1(S616D) (e, e'). These clones were cotransfected with DsRed-mito into cultured hippocampal neurons at DIV. Magnified images of straight mitochondrial morphology in white dotted boxes are shown at the bottom each panel. (b, c) Examples of neuron exhibiting punctate (b') or filamentous (c') form of YFP-hDrp1. (f) Proportion of neurons showing filamentous YFP-hDrp1. * $P < 0.05$, $n = 5$. (g) Proportion of neurons showing fragmented mitochondria. * $P < 0.05$, $n = 5$.

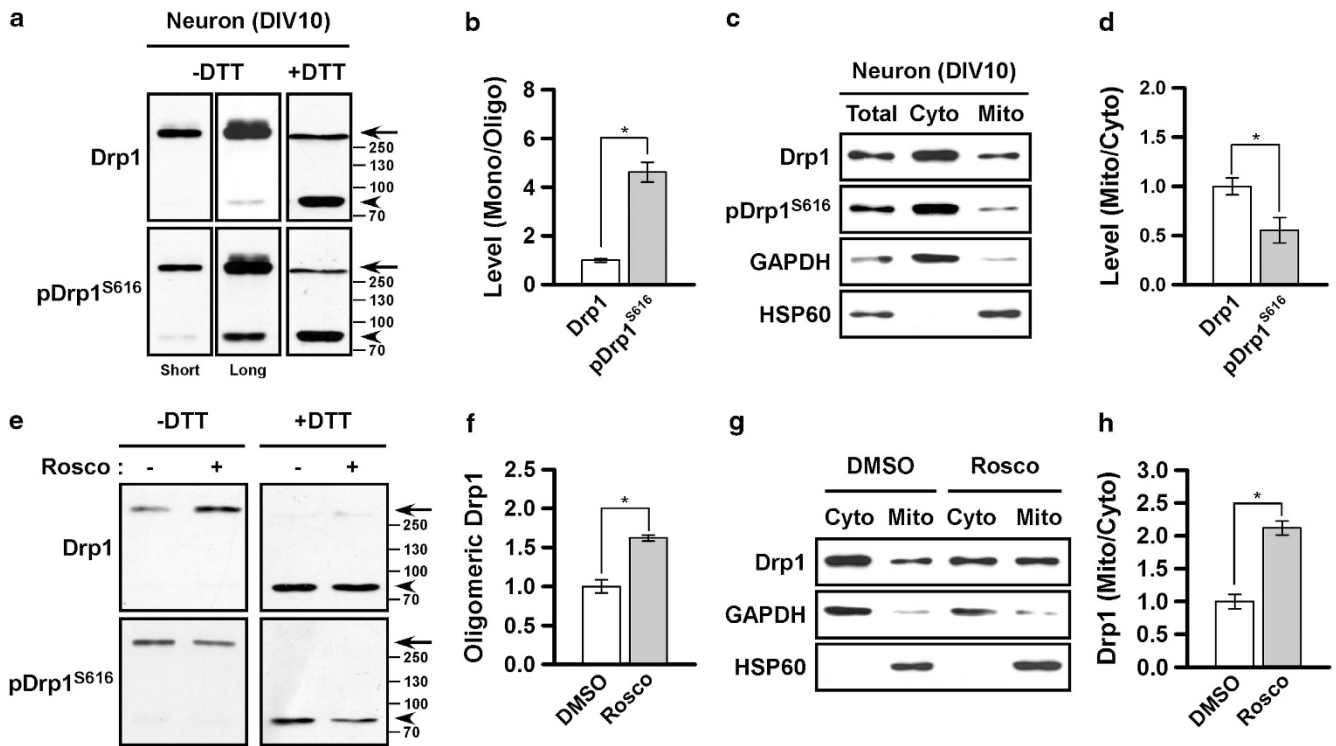


Figure 6 Drp1^{S616} phosphorylation inhibits oligomerization and mitochondrial translocation of Drp1. (a) Immunoblotting of monomeric (~80 kDa), tetrameric (~320 kDa) and the higher-ordered oligomeric forms of Drp1 and pDrp1^{S616} in cultured cortical neurons. SDS-PAGE with or without DTT was performed and followed by immunoblotting. Arrows and arrowheads indicate tetrameric or oligomeric Drp1 and monomeric Drp1, respectively. (b) Quantification of the ratio of pDrp1^{S616} versus total Drp1 in monomeric or oligomeric fractions. **P*<0.05, *n*=3. (c) Immunoblot of Drp1 and pDrp1^{S616} in cytosolic or mitochondrial fractions. Immunoblots of GAPDH and HSP60 were used as loading controls of mitochondrial and cytosolic fractions, respectively. (d) Quantification of the ratio of pDrp1^{S616} versus total Drp1 in cytosolic or mitochondrial fractions. **P*<0.05, *n*=3. (e) Immunoblot of monomeric, tetrameric and oligomeric forms of Drp1 and pDrp1^{S616} from cells treated with or without roscovitine (20 μM) for 2 h. Arrows and arrowheads indicate tetrameric or oligomeric Drp1 and monomeric Drp1, respectively. (f) Quantification of the ratio of Drp1 in monomeric and oligomeric fractions from cells treated with or without roscovitine. **P*<0.05, *n*=3. (g) Immunoblot of Drp1 and pDrp1^{S616} in cytosolic or mitochondrial fractions from cells treated with or without roscovitine (100 μM) for two hours. (h) Quantification of the ratio of Drp1 in cytosolic or mitochondrial fractions from cells treated with or without roscovitine. **P*<0.05, *n*=3.

For example, CDK5 can induce Drp1-mediated mitochondrial fragmentation during neuronal cell death³⁸ by promoting S-nitrosylation of Drp1.³⁹ However, the effect of CDK5 on Drp1 phosphorylation has not been examined under physiological conditions. In this study, we provide evidence that CDK5 promotes inhibitory phosphorylation of Drp1, which contributes to the mitochondrial elongation during the neuronal maturation. In fact, we failed to observe phosphorylation of Drp1 by CDK5 in an *in vitro* kinase assay (data not shown), which is contradictory to previous reports.^{22,38,39} Although we do not know the exact cause of this discrepancy, these results raise the possibility that the impact of CDK5 suppression in cells on Drp1 phosphorylation may be indirect.

Drp1^{S616} can be phosphorylated by multiple kinases. In addition to the CDK5, we found that ERK1/2 may be involved in the phosphorylation of Drp1^{S616} in neurons. In mitotic cells, CDK1 phosphorylates Drp1^{S616} during mitosis,²¹ whereas ERK1/2 phosphorylates Drp1^{S616} under high glucose conditions.²⁴ Drp1^{S616} can also be phosphorylated by PKCδ

in a hypertensive animal model.²³ It is believed that the phosphorylation of Drp1^{S616} activates the fission-promoting activity of Drp1. However, our current observations clearly showed that the induction of Drp1^{S616} phosphorylation is associated with mitochondrial fission in post-mitotic neurons. These data imply that the regulation of Drp1 activity by the phosphorylation in serine 616 may be dependent on the upstream kinases. Accordingly, we found that blockade of ERK1/2 by PD98059 resulted in mitochondrial elongation. Similar to Drp1^{S616}, cellular context-dependent alterations of the downstream effects have also been reported in the other phosphorylation site of Drp1, serine 637. Under starvation conditions, PKA-mediated phosphorylation serves as an inhibitory modification that inhibits GTPase activity, thereby inducing mitochondrial elongation.^{5,6} However, under hyperglycemic conditions in podocytes, rho-associated coiled-coil containing protein kinase 1 phosphorylates and conversely activates Drp1 by promoting mitochondrial translocation.⁴⁰ Another kinase, calmodulin-dependent protein kinase 1 alpha, also promotes Drp1 activity by

enhancing association with Fis1 in neuronal activation.⁴¹ Collectively, these observations suggest that the downstream effects of Drp1 phosphorylation are dependent on its upstream signaling, presumably due to the differential organization of protein complexes for the oligomerization and/or receptor interactions. Drp1 has multiple receptors on the mitochondrial outer membrane; thus, it is possible that different receptor bindings can promote or suppress the mitochondrial fission.¹²

Serine 616 is in the variable domain (VD), which resides between middle domain and GTPase effector domain.¹⁹ Recently, the VD has been shown to have a role in the regulation of Drp1 oligomerization.³² In addition, the VD contains multiple sumoylation sites⁴² and two phosphorylation sites, serine 616²¹ and 637,⁴³ suggesting that these post-translational modifications may modify oligomerization of Drp1. In this study, we found that a subset of YFP-hDrp1-expressing neurons exhibits extensive filament formation of Drp1, possibly due to excessive polymerization.³² A phosphorylation-defective mutant, YFP-hDrp1(S616A), has a stronger tendency to form filaments than wild type or phosphorylation-mimicking mutant form of Drp1, YFP-hDrp1(S616D), indicating that phosphorylation at serine 616 may induce conformational change of VD repressing the filament formation of Drp1.

Consistently, a large proportion of phosphorylated Drp1^{S616} was found in the monomeric pool compared with the total Drp1. Furthermore, suppression of Drp1^{S616} phosphorylation by roscovitine increased levels of tetrameric or oligomeric Drp1. Drp1 can be self-assembled and predominantly exists as tetramers *in vivo*.^{33,34} The tetrameric units can be further assembled into the higher-ordered spiral structure.⁴⁴ Therefore, our results demonstrate that CDK5-mediated phosphorylation appears to enhance the dissociation of Drp1 into monomeric forms from tetrameric or further oligomeric forms, which in turn reduces the fission-promoting activity. We also found that phosphorylated Drp1^{S616} was preferentially localized in the cytosol and that roscovitine induced mitochondrial translocation of Drp1. Because Drp1 is assembled into a high-ordered spiral structure on mitochondria,⁴⁵ reduced oligomerization of Drp1 by CDK5-dependent phosphorylation may cause reduced mitochondrial localization.

Recent reports have revealed that Drp1^{S616} phosphorylation by CDK1 inhibits the sequestration of Drp1 on the microtubule, thereby promoting mitochondrial translocation of Drp1 and subsequent mitochondrial fragmentation.^{21–24} In fact, overexpression of wild-type, phosphor-defective and phosphor-mimic forms of YFP-hDrp1 did not significantly influence the mitochondrial morphology in interphase cells, although phosphorylation of Drp1^{S616} markedly altered mitochondrial morphology in mitotic cells.⁴⁶ Therefore, these lines of evidence consistently suggest that the biological impact of phosphorylation of Drp1^{S616} is dependent on the upstream kinases and the cellular contexts.

Collectively, our results suggest that CDK5 has a significant role in the regulation of mitochondrial morphology via

reduction in the oligomerization activity of Drp1 in post-mitotic neurons.

ACKNOWLEDGEMENTS

This research was supported by the Brain Research Program through the National Research Foundation (NRF) funded by the Korean Ministry of Science, ICT & Future Planning (NRF-2012M3A9C6049933, NRF-2011-0019212, and NRF-2013R1A1A3011896).

- 1 Knott AB, Perkins G, Schwarzenbacher R, Bossy-Wetzel E. Mitochondrial fragmentation in neurodegeneration. *Nat Rev Neurosci* 2008; **9**: 505–518.
- 2 Li H, Alavian KN, Lazrove E, Mehta N, Jones A, Zhang P *et al*. A Bcl-xL-Drp1 complex regulates synaptic vesicle membrane dynamics during endocytosis. *Nat Cell Biol* 2013; **15**: 773–785.
- 3 Chan DC. Mitochondrial fusion and fission in mammals. *Annu Rev Cell Dev Biol* 2006; **22**: 79–99.
- 4 Tondera D, Grandemange S, Jourdain A, Karbowski M, Mattenberger Y, Herzig S *et al*. SLP-2 is required for stress-induced mitochondrial hyperfusion. *Embo J* 2009; **28**: 1589–1600.
- 5 Gomes LC, Di Benedetto G, Scorrano L. During autophagy mitochondria elongate, are spared from degradation and sustain cell viability. *Nat Cell Biol* 2011; **13**: 589–598.
- 6 Rambold AS, Kostecky B, Elia N, Lippincott-Schwartz J. Tubular network formation protects mitochondria from autophagosomal degradation during nutrient starvation. *Proc Natl Acad Sci USA* 2011; **108**: 10190–10195.
- 7 Mai S, Klivenberg M, Auburger G, Bereiter-Hahn J, Jendrach M. Decreased expression of Drp1 and Fis1 mediates mitochondrial elongation in senescent cells and enhances resistance to oxidative stress through PINK1. *J Cell Sci* 2010; **123**(Pt 6), 917–926.
- 8 Cheng A, Wan R, Yang JL, Kamimura N, Son TG, Ouyang X *et al*. Involvement of PGC-1 α in the formation and maintenance of neuronal dendritic spines. *Nat Commun* 2012; **3**: 1250.
- 9 Frank S, Gaume B, Bergmann-Leitner ES, Leitner WW, Robert EG, Catez F *et al*. The role of dynamin-related protein 1, a mediator of mitochondrial fission, in apoptosis. *Dev Cell* 2001; **1**: 515–525.
- 10 Montessuit S, Somasekharan SP, Terrones O, Lucken-Ardjomande S, Herzig S, Schwarzenbacher R *et al*. Membrane remodeling induced by the dynamin-related protein Drp1 stimulates Bax oligomerization. *Cell* 2010; **142**: 889–901.
- 11 Song Z, Ghojani M, McCaffery JM, Frey TG, Chan DC. Mitofusins and OPA1 mediate sequential steps in mitochondrial membrane fusion. *Mol Biol Cell* 2009; **20**: 3525–3532.
- 12 Dikov D, Reichert AS. How to split up: lessons from mitochondria. *Embo J* 2011; **30**: 2751–2753.
- 13 Ingerman E, Perkins EM, Marino M, Mears JA, McCaffery JM, Hinshaw JE *et al*. Dnm1 forms spirals that are structurally tailored to fit mitochondria. *J Cell Biol* 2005; **170**: 1021–1027.
- 14 Mears JA, Lackner LL, Fang S, Ingerman E, Nunnari J, Hinshaw JE. Conformational changes in Dnm1 support a contractile mechanism for mitochondrial fission. *Nat Struct Mol Biol* 2011; **18**: 20–26.
- 15 Ishihara N, Nomura M, Jofuku A, Kato H, Suzuki SO, Masuda K *et al*. Mitochondrial fission factor Drp1 is essential for embryonic development and synapse formation in mice. *Nat Cell Biol* 2009; **11**: 958–966.
- 16 Wakabayashi J, Zhang Z, Wakabayashi N, Tamura Y, Fukaya M, Kensler TW *et al*. The dynamin-related GTPase Drp1 is required for embryonic and brain development in mice. *J Cell Biol* 2009; **186**: 805–816.
- 17 Li Z, Okamoto K, Hayashi Y, Sheng M. The importance of dendritic mitochondria in the morphogenesis and plasticity of spines and synapses. *Cell* 2004; **119**: 873–887.
- 18 Choi SY, Kim JY, Kim HW, Cho B, Cho HM, Oppenheim RW *et al*. Drp1-mediated mitochondrial dynamics and survival of developing chick motoneurons during the period of normal programmed cell death. *FASEB J* 2013; **27**: 51–62.
- 19 Elgass K, Pakay J, Ryan MT, Palmer CS. Recent advances into the understanding of mitochondrial fission. *Biochim Biophys Acta* 2013; **1833**: 150–161.

- 20 Cho B, Choi SY, Cho HM, Kim HJ, Sun W. Physiological and pathological significance of dynamin-related protein 1 (Drp1)-dependent mitochondrial fission in the nervous system. *Exp Neurol* 2013; **22**: 149–157.
- 21 Taguchi N, Ishihara N, Jofuku A, Oka T, Mihara K. Mitotic phosphorylation of dynamin-related GTPase Drp1 participates in mitochondrial fission. *J Biol Chem* 2007; **282**: 11521–11529.
- 22 Strack S, Wilson TJ, Cribbs JT. Cyclin-dependent kinases regulate splice-specific targeting of dynamin-related protein 1 to microtubules. *J Cell Biol* 2013; **201**: 1037–1051.
- 23 Qi X, Disatnik MH, Shen N, Sobel RA, Mochly-Rosen D. Aberrant mitochondrial fission in neurons induced by protein kinase C(δ) under oxidative stress conditions in vivo. *Mol Biol Cell* 2011; **22**: 256–265.
- 24 Yu T, Jhun BS, Yoon Y. High-glucose stimulation increases reactive oxygen species production through the calcium and mitogen-activated protein kinase-mediated activation of mitochondrial fission. *Antioxid Redox Signal* 2011; **14**: 425–437.
- 25 Almeida A, Bolanos JP, Moreno S. Cdh1/Hct1-APC is essential for the survival of postmitotic neurons. *J Neurosci* 2005; **25**: 8115–8121.
- 26 Su SC, Tsai LH. Cyclin-dependent kinases in brain development and disease. *Annu Rev Cell Dev Biol* 2011; **27**: 465–491.
- 27 Cho B, Choi SY, Park OH, Sun W, Geum D. Differential expression of BNIP family members of BH3-only proteins during the development and after axotomy in the rat. *Mol Cell* 2012; **33**: 605–610.
- 28 Kim WR, Chun SK, Kim TW, Kim H, Ono K, Takebayashi H *et al*. Evidence for the spontaneous production but massive programmed cell death of new neurons in the subcallosal zone of the postnatal mouse brain. *Eur J Neurosci* 2011; **33**: 599–611.
- 29 Chang DT, Reynolds IJ. Mitochondrial trafficking and morphology in healthy and injured neurons. *Prog Neurobiol* 2006; **80**: 241–268.
- 30 Chang DT, Reynolds IJ. Differences in mitochondrial movement and morphology in young and mature primary cortical neurons in culture. *Neuroscience* 2006; **141**: 727–736.
- 31 Patrick GN, Zukerberg L, Nikolic M, de la Monte S, Dikkes P, Tsai LH. Conversion of p35 to p25 deregulates Cdk5 activity and promotes neurodegeneration. *Nature* 1999; **402**: 615–622.
- 32 Strack S, Cribbs JT. Allosteric modulation of Drp1 assembly and mitochondrial fission by the variable domain. *J Biol Chem* 2012.
- 33 Zhu PP, Patterson A, Stadler J, Seeburg DP, Sheng M, Blackstone C. Intra- and intermolecular domain interactions of the C-terminal GTPase effector domain of the multimeric dynamin-like GTPase Drp1. *J Biol Chem* 2004; **279**: 35967–35974.
- 34 Shin HW, Takatsu H, Mukai H, Munekata E, Murakami K, Nakayama K. Intermolecular and interdomain interactions of a dynamin-related GTP-binding protein, Dnm1p/Vps1p-like protein. *J Biol Chem* 1999; **274**: 2780–2785.
- 35 Yuan Z, Becker EB, Merlo P, Yamada T, DiBacco S, Konishi Y *et al*. Activation of FOXO1 by Cdk1 in cycling cells and postmitotic neurons. *Science* 2008; **319**: 1665–1668.
- 36 Tomizawa K, Sunada S, Lu YF, Oda Y, Kinuta M, Ohshima T *et al*. Cophosphorylation of amphiphysin I and dynamin I by Cdk5 regulates clathrin-mediated endocytosis of synaptic vesicles. *J Cell Biol* 2003; **163**: 813–824.
- 37 Tan TC, Valova VA, Malladi CS, Graham ME, Berven LA, Jupp OJ *et al*. Cdk5 is essential for synaptic vesicle endocytosis. *Nat Cell Biol* 2003; **5**: 701–710.
- 38 Meuer K, Suppanz IE, Lingor P, Planchamp V, Goricke B, Fichtner L *et al*. Cyclin-dependent kinase 5 is an upstream regulator of mitochondrial fission during neuronal apoptosis. *Cell Death Differ* 2007; **14**: 651–661.
- 39 Qu J, Nakamura T, Cao G, Holland EA, McKercher SR, Lipton SA. S-Nitrosylation activates Cdk5 and contributes to synaptic spine loss induced by beta-amyloid peptide. *Proc Natl Acad Sci USA* 2011; **108**: 14330–14335.
- 40 Wang W, Wang Y, Long J, Wang J, Haudek SB, Overbeek P *et al*. Mitochondrial fission triggered by hyperglycemia is mediated by ROCK1 activation in podocytes and endothelial cells. *Cell Metab* 2012; **15**: 186–200.
- 41 Han XJ, Lu YF, Li SA, Kaitsuka T, Sato Y, Tomizawa K *et al*. CaM kinase I alpha-induced phosphorylation of Drp1 regulates mitochondrial morphology. *J Cell Biol* 2008; **182**: 573–585.
- 42 Figueroa-Romero C, Iniguez-Lluhi JA, Stadler J, Chang CR, Arnoult D, Keller PJ *et al*. SUMOylation of the mitochondrial fission protein Drp1 occurs at multiple nonconsensus sites within the B domain and is linked to its activity cycle. *FASEB J* 2009; **23**: 3917–3927.
- 43 Cribbs JT, Strack S. Reversible phosphorylation of Drp1 by cyclic AMP-dependent protein kinase and calcineurin regulates mitochondrial fission and cell death. *EMBO Rep* 2007; **8**: 939–944.
- 44 Ramachandran R, Surka M, Chappie JS, Fowler DM, Foss TR, Song BD *et al*. The dynamin middle domain is critical for tetramerization and higher-order self-assembly. *Embo J* 2007; **26**: 559–566.
- 45 Labrousse AM, Zappaterra MD, Rube DA, van der Bliet AM. C. elegans dynamin-related protein DRP-1 controls severing of the mitochondrial outer membrane. *Mol Cell* 1999; **4**: 815–826.
- 46 Cereghetti GM, Stangherlin A, Martins de Brito O, Chang CR, Blackstone C, Bernardi P *et al*. Dephosphorylation by calcineurin regulates translocation of Drp1 to mitochondria. *Proc Natl Acad Sci USA* 2008; **105**: 15803–15808.



This work is licensed under a Creative Commons Attribution-NonCommercial-ShareAlike 3.0 Unported License. The images or other third party material in this article are included in the article's Creative Commons license, unless indicated otherwise in the credit line; if the material is not included under the Creative Commons license, users will need to obtain permission from the license holder to reproduce the material. To view a copy of this license, visit <http://creativecommons.org/licenses/by-nc-sa/3.0/>

Supplementary Information accompanies the paper on Experimental & Molecular Medicine website (<http://www.nature.com/emm>)